frontiers | Frontiers in Nanotechnology

TYPE Original Research
PUBLISHED 20 May 2024
DOI 10.3389/fnano.2024.1352287

OPEN ACCESS

EDITED BY
Neha Kaushik,
University of Suwon, Republic of Korea

REVIEWED BY
Satheesh kumar Balu,
Saveetha Dental College And Hospitals, India
Yashika Rustagi,
Dana–Farber Cancer Institute, United States

*CORRESPONDENCE
Elena Alexander,
ei2169@columbia.edu

RECEIVED 07 December 2023
ACCEPTED 26 April 2024
PUBLISHED 20 May 2024

CITATION
Alexander E and Leong KW (2024), Immunomodulatory effects of laser-synthesized nanodiamonds on peripheral blood mononuclear cells: evaluation of unconjugated, PEGylated, and antibody-conjugated formulations.
Front. Nanotechnol. 6:1352287.
doi: 10.3389/fnano.2024.1352287

Immunomodulatory effects of laser-synthesized nanodiamonds on peripheral blood mononuclear cells: evaluation of unconjugated, PEGylated, and antibody-conjugated formulations

Elena Alexander* and Kam W. Leong

Department of Biomedical Engineering, Columbia University, New York City, NY, United States

The application of laser-synthesized nanodiamonds (LNDs) is of great interest to biomedical researchers and drug developers because this emerging method of synthesis yields nanodiamonds of consistent size (<5 nm diameter) and surface chemistry that can be functionalized to perform a staggering range of highly specialized tasks. The present study assessed the threshold at which LNDs in various conjugations and concentrations triggered immune responses and cytotoxicity in peripheral mononuclear blood cells from healthy donors, as assessed by changes in ATP concentrations and induced secretion of the cytokines IFN-γ, IL-6 and TNF-α. Conjugations assessed were raw (unconjugated) NDs, PEGylated (PEG5k-NDs), and antibody conjugated to goat anti-mouse antibodies (IgG-NDs). Concentrations of each conjugation were prepared and tested at 50.0, 10.0, 2.0, 0.4, and 0.08 μg/mL. Results showed that pegylated and raw NDs were well tolerated, with the indicators of inflammation or minimal cytotoxicity emerging only at the highest concentrations tested (50.0 μg/mL). IgG-NDs showed signs of inflammatory responses at the two highest concentrations tested (10.0 and 50.0 μg/mL). There was some evidence that the dilutant vehicle used for ND suspension may have contributed to the immune response. All three ND configurations increased ATP concentration in a dose-dependent manner, up to a concentration of 10.0 μg/mL. At the highest concentration (50.0 μg/mL), the ND solutions showed minimal signs of cytotoxicity. Conclusion from this testing suggest that LNDs are likely to offer substantial utility in biomedical applications because of their capacity to evade the immune response at concentrations at least as high as 2.0 μg/mL and potentially up to 50.0 μg/mL.

KEYWORDS

nanodiamond, biomedical application, immune response, nanomaterials, carbon-based nanomaterials (CBNs)

1 Introduction

Nanodiamonds (NDs) describe a family of carbon-based nanomaterials (i.e., diameter <100 nm) with the same sp^3 lattice structure that gives natural diamonds their exceptional hardness and electrical insulating properties. The outer surface of NDs, however, is composed of unpaired carbon atoms in the sp^2 configuration, which makes this novel material relatively easy to manipulate and customize for a variety of highly specific functions (Gao et al., 2019; Reina et al., 2019; Chang et al., 2022). Interest in NDs for biomedical applications has grown dramatically in the past decade, owing largely to their high biocompatibility and easily customizable surface chemistry. Of all known carbon nanomaterials—e.g., nanotubes and fullerenes—NDs have the highest biocompatibility in addition to excellent stability *in vivo*, making them exciting candidates for nanomedical applications (Sadat et al., 2022).

1.1 Nanodiamonds and immunogenicity

Among the many lines of investigation being pursued for deploying NDs to improve human health is their capacity to modulate the immune system. Studies have demonstrated the capacity of NDs to elicit highly specific immune responses by affixing different antibodies and small molecules to their surface (Suarez-Kelly et al., 2021; Paladhi et al., 2022). A few of the many examples include enhanced proliferation of $CD4^+$ and $CD8^+$ T-cells (Ghoneum et al., 2014), B-lymphocytes (Huang et al., 2017; Suarez-Kelly et al., 2017), macrophages (Pentecost et al., 2019), and neutrophils (Chang et al., 2003).

Conversely, many potential applications of NDs seek to minimize or eliminate the immune response to particles so that the latter can perform a particular function unimpeded. Examples include intravenous injection of functionalized fluorescent NDs for bioimaging (Kaçar and Erden, 2020; Montes et al., 2020; van der Laan et al., 2020; Lin et al., 2022; Sharmin et al., 2022; Li et al., 2023) or accumulation of functionalized NDs around damaged tissues (e.g., cardiac, neural) to induce stem-cell repair (Ansari et al., 2016; Alexander et al., 2019; Taylor et al., 2019; Liu et al., 2021).

At the heart of ND interaction with the immune system are Adenosine Triphosphate (ATP) and cytokines. ATP, beyond its role as the cellular "energy currency," functions as a signaling molecule that influences cellular processes, including metabolism, stress responses, and immune signaling (Zimmermann, 2000; Di Virgilio et al., 2018). High ATP levels might indicate increased metabolic activity or stress responses, while low levels could suggest energy depletion or impaired metabolic function (Shao et al., 2018).

Cytokines, as key signaling molecules, play significant roles in mediating immunity and inflammation. Elevated cytokine levels typically signal an active immune response, possibly due to infection or inflammation, and might also indicate autoimmune processes. Conversely, low cytokine levels can point to immune deficiencies or regulatory dysfunctions, highlighting the balance between pro-inflammatory and anti-inflammatory responses as a critical factor in health and disease (Iwamoto et al., 2014).

The interaction between ATP and cytokines is particularly intriguing, as ATP can act as an extracellular signaling molecule influencing cytokine production. This crosstalk is evident in situations of cellular stress or damage, where ATP is released and can trigger inflammatory responses through cytokine production, demonstrating the interconnectedness of energy metabolism and immune responses (Vultaggio-Poma et al., 2020).

In pathophysiological conditions, such as cancer and autoimmune diseases, the dysregulation of ATP production and cytokine secretion is a common feature. In cancer, altered ATP metabolism supports uncontrolled cell proliferation, while in autoimmune diseases, cytokine imbalances drive inflammation and tissue damage, pointing to the potential of targeting these pathways for therapeutic interventions.

Understanding the intricate relationships between ATP levels, cytokine profiles, and disease states could unveil new therapeutic targets and biomarkers for disease detection and monitoring. This knowledge emphasizes the importance of a comprehensive analysis of ATP and cytokine concentrations for developing innovative therapeutic strategies and improving disease management (Kalyanaraman, 2017).

This study aims to dissect the immunomodulatory effects of LNDs, characterized by their purity and consistent nanoscale dimensions, on peripheral blood mononuclear cells (PBMCs). Through examining changes in ATP concentrations and the secretion of key cytokines (IFN-γ, IL-6, TNF-α), we seek to elucidate the mechanisms through which LNDs interact with cellular metabolism and the immune response, contributing to the broader understanding of NDs in biomedical applications.

1.2 Findings and overview

The present study investigated the immunomodulatory effects of three configurations of laser-synthesized NDs (LNDs, diameter <5 nm) on peripheral blood mononuclear cells (PBMCs) from healthy donors. Specifically, NDs were tested as unconjugated (raw-NDs, in-vehicle only), PEGylated (PEG5k-NDs), and antibody conjugated (IgG-NDs).

As measured by changes in ATP concentrations and induced secretion of the cytokines IFN-γ, IL-6, and TNF-α, the pegylated and raw NDs were well tolerated by PBMCs with no indication of inflammation or cytotoxicity, except at the highest concentrations tested (50 μg/mL). PBMCs incubated with IgG-NDs showed signs of inflammatory responses at ND concentrations of 10 and 50 μg/mL. However, there was some evidence that the dilutant vehicle used for ND suspension may have exacerbated the elevation in IL-6 and TNF-α, in addition to stimulating ATP production and cellular proliferation.

PBMC incubation with all three ND formulations resulted in increased ATP concentration in a dose-dependent manner, up to a concentration of 10 μg/mL. At the next-highest concentration assessed (50 μg/mL), the ND solutions showed signs of non-specific cytotoxicity with increases in ATP.

At ND concentrations of 0.08, 0.4, and 2.0 μg/mL, there were no signs of either cytotoxicity or inflammatory response in PBMCs. Taken together, these findings suggest LNDs—including LNDs conjugated to antibodies—may be able to evade the immune response at concentrations at least as high as 2.0 μg/mL and potentially as high as 10 μg/mL.

TABLE 1 Treatment groups and related readouts.

Condition	Dose	Readouts
Media alone	N/A	ATP Glo assay
Vehicle 1 (dH_2O)	10, 2% and 0.4%	IL-6, TNFα, and IFN-γ quantification: Multiplex
Vehicle 2 (custom conjugate diluent)	10, 2% and 0.4%	
Muronomab (OKT3)	5 μg/mL	
ANC28.1	5 μg/mL	
IgG1	5 μg/mL	
Raw-NDs	50, 10, 2, 0.4, 0.08 μg/mL	
PEG5k-NDs		
IgG-NDs		

dH_2O = sterile, filtered deionized water; N/A = not applicable; ND, nanodiamond; OKT3 = plate-bound anti-CD3, stimulus.
Note: Custom conjugant dilutant consisted of 1*PBS +10% FBS; (see Section 2.2).

2 Materials and methods

2.1 Background on laser-synthesized nanodiamonds

LNDs differ from more common forms of NDs (e.g., detonation NDs [DNDs] or high-temperature high-pressure NDs [HTHP-NDs]) in that they are virtually devoid of impurities and have a smaller diameter that consistently ranges from 4 7 nm when compared with DNDs (4–100 nm) 21 and HTHP-NDs (≥40 nm and irregularly shaped) (Baidakova et al., 2013; Perevedentseva et al., 2015) 22. LNDs were chosen for this study because they offer some advantages for highly sensitive bio-applications: higher purity, better structural and spectroscopic properties, higher paramagnetism, easier control of surface chemistry (due to the absence of metal and graphite impurities), and lower cytotoxicity (Peer et al., 2007; Perevedentseva et al., 2015) 22, 23. Recent improvements in LND synthesis yield NDs with a diameter consistently <5 nm and a high purity—i.e., carbon >94% when compared with DNDs that are generally <86% carbon (Perevedentseva et al., 2015). 22.

2.2 Study design

This study evaluated NDs in three conjugations (raw/unconjugated, PEG5k-NDs, and IgG-NDs) for cytotoxicity and immunogenicity in human PBMCs from healthy donors. Endpoints were measured by relative ATP concentration and induced secretion of the cytokines IFN-γ, IL-6, and TNF-α.

NDs were prepared and tested at final assay concentrations of 50, 10, 2, 0.4, and 0.08 μg/ml. A serial dilution of NDs was prepared in assay media with sterile-filtered deionized water (SFDI) or custom conjugate dilutant, resulting in vehicle concentrations of 10%, 2%, 0.4%, 0.08%, and 0.016%. The custom conjugate dilutant consisted of 10% fetal bovine serum in phosphate-buffered solution (abbreviated as 1*PBS +10% FBS). Vehicle controls were tested at 10%, 2%, and 0.4%.

PBMCs were incubated in the presence of media only (plate-bound anti-CD3 stimulus [OKT3], soluble anti-CD28 stimulus, or antibody isotype control) for 72 h. PBMCs were then incubated with NDs at the five assay concentrations (i.e., 50.0, 10.0, 0.4, and 0.08 μg/mL) for 72 h. Each condition was plated in triplicate. After 72 h, supernatants were collected. Cells were lysed, and ATP quantified as a measure of cell number by CellTiter-Glo assay. IFN-γ, IL-6 and TNF-α cytokine concentrations in supernatant were analyzed by multiplex assay (Luminex®). Table 1 provides an overview of all conjugations, doses, and readouts used in the study.

Table 2 provides an overview of the ND conjugations tested and their relevant parameters.

2.3 Preparation and storage of nanodiamonds

Laser-synthesized ND powder with an average grain size <5 nm was obtained from Ray Techniques Ltd. Stock NDs were suspended by sonication before serial dilution in assay media (RPMI containing 2% HEPES, 2% L-Glutamine, and 10% human AB serum) and then incubated with 200,000 PBMCs. Final concentrations of NDs tested were 50 μg/mL, 10 μg/mL, 2 μg/mL, 0.4 μg/mL, and 0.08 μg/mL of raw NDs, PEG5k-NDs and IgG-NDs and 10%, 2%, and 0.4% of custom conjugate diluent and SFDI. Controls consisted of 1 μg/well of anti-CD3, anti-CD28 or isotype control. Cells were incubated in a humidified chamber at 5% CO_2 for 72 h. With the exception of probe sonication, the nanodiamonds were handled in a laminar flow hood to minimize exposure to contamination.

Raw NDs served as a control to determine what effects the ND themselves may have on the cells being studied. Analysis of this source of ND revealed that carboxylic acid groups served as a ready handle for functionalizing via an amide bond using standard EDC/NHS chemistry. Amino-mPEG5k was conjugated to the ND via the NH_2 end group, forming a stable amide bond. The PEG was methoxy terminated to introduce PEG without any additional functional groups. PEG is often coated onto the ND to improve nanoparticle circulation and shield the nanoparticle from the immune system. The length of the PEG was chosen as an intermediate between smaller and larger commercially available PEG lengths and matched well with

TABLE 2 Overview of ND conjugations used for assay testing.

Description	Number, Mean (nm)	PDI	pH	Zeta (mV)	Std dev Zeta
Raw ND in SFDI	160	0.029	4.8	38	1
ND-PEG5k in SFDI	320	0.38	5.2	36.5	0.7
ND-Ab in buffer	370	0.29	7.7	−28	0.7

Ab, antibody; dev, deviation; ND, nanodiamond; PDI; PEG, pegylated; SFDI, spatial frequency domain imaging.

the size of the ND. Goat anti-mouse antibody was chosen as a model antibody because it easily demonstrated functionality once conjugated to the ND via lateral flow assay (LFA) and was more likely to induce an immune response than the other two ND samples tested.

2.3.1 Preparation of ND suspension

Initial ND suspension was performed by adding 10 mg of ND powder to a sterile scintillation vial then adding 10 g of water. The vial was then sealed and placed in a bath sonicator until all NDs had been wetted (approximately 10 min). The ND suspension was disaggregated using a Sonic Ruptor 250™ from Omni Inc® using an OR-T-156 5/32 probe sonicator set at 40% max power (80% max power for probe size) with 60% pulse in a 0°C bath for 6 h. Raw NDs were NDs that only underwent the above preparation via probe sonication without further modification. The particles were characterized via UV-Vis, dynamic light scattering (DLS), zeta potential, and transmission electron microscope (TEM) (Figure 1).

2.3.2 ND PEGylation

Suspended NDs were then transferred to a 15 mL conical tube, and the pH adjusted by adding 25 µL 0.1 M NaOH. Freshly prepared aliquots of EDC[1] and NHS[2] at a concentration of 10 mg/mL (200 µL and 400 µL, respectively) were added to the NDs. The NDs were then incubated end-over-end on a rotator for 30 min. The sample was transferred to a 100 kDa MWCO[3] spin filter and spun at 1,452 rcf for 5 min. The material was transferred to a new 15 mL conical tube and resuspended in 10 mL of SFDI water + 25 µL 0.1 M NaOH. Then, 20 µL of mPEG5k-NH2 (10 mg/mL) was added to the ND suspension and allowed to incubate end-over-end at room temperature for 90 min. Hydroxylamine (50 µL) was added to quench any remaining activated EDC/NHS sites, allowing the sample to incubate for 10 min. The sample was transferred to a new spin filter and spun at 1,452 rcf for 5 min. The filtrate was removed, and the NDs were washed with an additional 5 mL SFDI two more times. PEGylated NDs were transferred to a new 15 mL tube and resuspended with 8 mL SFDI. PEGylated NDs were characterized via UV-vis, DLS, zeta potential, FTIR[4], and TEM and were stored at 4°C.

2.3.3 Antibody conjugation

ND carboxylate groups were again activated with EDC/NHS, as described above, to a 1 mg/mL suspension of sonicated ND in a 15 mL conical tube. Then, 10 µg purified antibody was added to the activated ND and incubated at room temperature for 1 h, followed by quenching with 50 µL hydroxylamine, with an additional 10-min incubation. Then, 100 µL 10% bovine serum albumin (BSA) was added to the ND, and the reaction mixture was incubated at room temp for an additional 10 min. The NDs were centrifuged at 5,000 rcf for 5 min, and the supernatant was removed. The NDs were resuspended in reaction buffer (5 mM sodium phosphate, 0.55 PEG20k, pH 7.4) and incubated on a rotator for 10 min, then centrifuged again at 5,000 rcf for 5 min. The NDs were resuspended in 8 mL of conjugate diluent (0.5× phosphate buffered saline, 0.5% casein, 0.5% BSA, 1% Tween 20™).

Goat-anti-mouse antibody-conjugated NDs (IgG-NDs) were characterized via UV-vis, DLS, zeta potential, and LFA. For LFA to test for the presence of functional Ab conjugated to ND, test strips were used with a negative control line of donkey-anti rabbit located 6 mm below the test line of mouse IgG. Only the test line was visible after running LFA with IgG-NDs. IgG-NDs were stored at 4°C.

2.4 Compunds and reagents tested

SFDI was used and additionally filtered through a 0.22 µm sterile filter. mPEG-5k-Amine was purchased from LyasanBio. EDC (1-ethyl-3-(3-dimethylaminopropyl) carbodiimide), sulfo-NHS (N-hydroxysulfosuccinimide), and hydroxylamine (50% in water) were purchased from Sigma-Aldrich. Goat anti-mouse antibodies (IgG Fc) were purchased from Lampire Biological Laboratories®. Reagents were used as received unless otherwise indicated.

2.5 Samples and assays used for testing

2.5.1 Blood sample collection

50–60 mL of whole blood was collected from healthy donors in sodium heparin vacutainer tubes. PBMCs were isolated from whole blood via density gradient centrifugation. Whole blood was diluted 1:1 in Ca^{2+}/Mg^{2+}-free HHBSS[5] before layering onto Histopaque® 1119. Blood was centrifuged, and contaminating red blood cells were removed with ammonium chloride potassium (ACK) lysis buffer.

1 EDC=(1-ethyl-3-(3-dimethylaminopropyl)carbodiimide hydrochloride).

2 NHS = N-hydroxysuccinimide.

3 MWCO = molecular weight cutoff.

4 FTIR = Fourier transform infrared spectroscopy.

5 HHBSS = HEPES-buffered Hanks balanced salt solution; HEPES = N-2-hydroxyethylpiperazine-N′-2-ethanesulfonic acid.

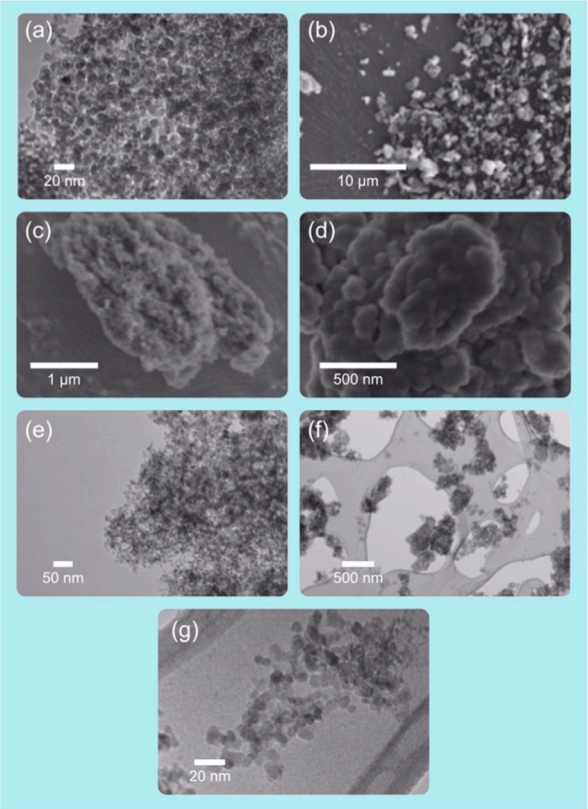

FIGURE 1
Images of NDs at various resolutions as they appear when captured with scanning-electron and transmission-electron microscopes. Laser synthesized nanodiamonds. Images **(A,E,F,G)** TEM. Images **(B–D)** SEM. Original illustration and images.

After isolation, viable PBMCs were counted using acridine orange/propidium iodide (AO/PI) viability stain and a Luna™ cell counter.

2.5.2 ATP Assay

Following a 72-h incubation, the plates were centrifuged, and supernatants were collected and frozen for Luminex analysis. The cells were mixed thoroughly before lysis with 100 µL of Promega Cell Titer Glo 2.0™ reagent. Luminescence was read on a luminometer to measure ATP concentration.

2.5.3 Luminex Assay

Concentrations of IFN-γ, IL-6, and TNF-α in cell culture supernatants were measured using a Bio-plex Luminex platform (BioRad), according to manufacturer's protocol.

2.6 Imaging tools

Nanodiamond grain and cluster sizes were imaged using a JEOL 1010 transmission electron microscope (TEM) equipped with a CCD camera for image capture. Dispersions of nanodiamonds were dried onto carbon-coated TEM grids prior to imaging. Dynamic light scattering (DLS) and zeta potential measurements were obtained from nanodiamond dispersions using a Malvern® Zetasizer Nano ZS™. UV-visible optical spectroscopy was obtained from nanodiamond solutions using an Agilent® 8453 spectrometer. Fourier transform infrared (FTIR) spectra were obtained from dried powder samples in attenuated-total reflectance mode and measured on a PerkinElmer® Spectrum 100™ UATR-FTIR.

3 Results

3.1 ATP levels in peripheral blood mononuclear cells

Incubation for 72 h with anti-CD3 treatment of PBMCs from all donors resulted in increased ATP concentration compared with media controls, which was indicative of increased cell proliferation (Figure 2; left panel). Furthermore, a slight increase in ATP concentration with anti-CD28 treatment but not with isotype control was detected. This suggests that the PBMCs from all donors were suitably plated for this experiment and were capable of proliferating with the control stimulation.

Of the vehicle controls tested, dH_2O had no effect on ATP at concentrations of 0.4%, 2%, or 10% and did not differ notably from the media control. The custom conjugate diluent appeared to reduce ATP concentration when tested at 10% (equivalent to 50 µg/mL). At 2% concentration, the custom conjugate diluent appeared to slightly increase the cell number, while there was no effect at 0.4%. ATP concentrations after 72-h incubation with any of the three ND formulations were very similar (Figure 2; right panel). Cells incubated with all three NDs appeared to show a modest, but concentration-dependent increase in ATP concentration between 80 ng/mL and 10 µg/mL. At 50 µg/mL, there was a negligible difference in ATP concentration when cells were treated with any of the three NDs or with media alone. Mean ATP concentrations are presented below. ATP concentrations from individual donors are presented in Section 6.1 in Supplementary Data.

This figure depicts the mean adenosine triphosphate (ATP) levels in PBMCs from three healthy donors, treated with different concentrations of nanodiamond (ND) formulations. The left panel shows control conditions, while the right panel displays responses to various ND conjugations. Data illustrate a dose-dependent increase in ATP concentration, indicating cell viability across the tested ND concentrations. Error bars represent standard error of the mean (SEM). Abbreviations: dH2O = sterile, filtered deionized water; h = hour; ND = nanodiamond; PBMC = peripheral blood mononuclear cells; SEM = standard error of the mean.

3.2 Cytokine concentrations in cell culture supranatants

PBMCs from all donors showed strong secretion of IFN-γ following anti-CD3 stimulation (Figure 3; top-left panel). There was no detectable induction of IFN-γ when cells were treated with anti-CD28, IgG1 isotype, or media alone. This suggests there was little background activation in the CD3-expressing cells when they were not activated by a specific stimulus.

Similar to IFN-γ, IL-6 was undetectable in media only-treated cells or with isotype control (Figure 3; top-center panel). When cells

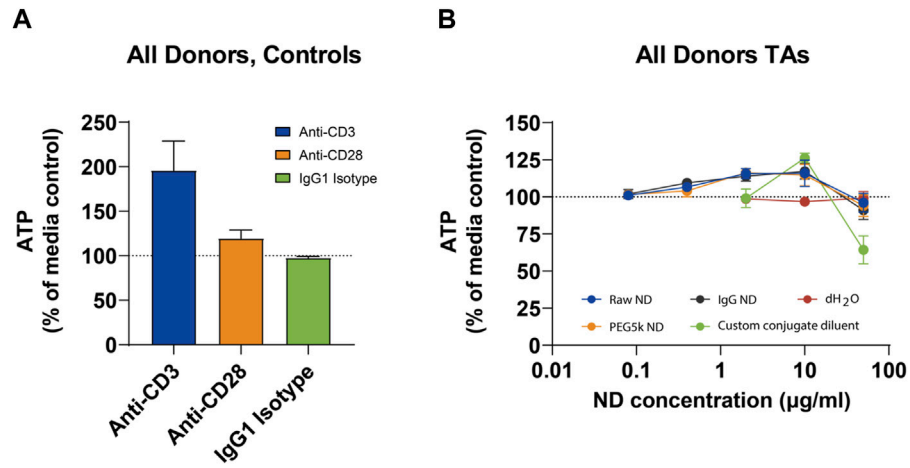

FIGURE 2
Mean ATP Levels in Peripheral Blood Mononuclear Cells in Controls **(A)** and Nanodiamond Conjugations **(B)**.

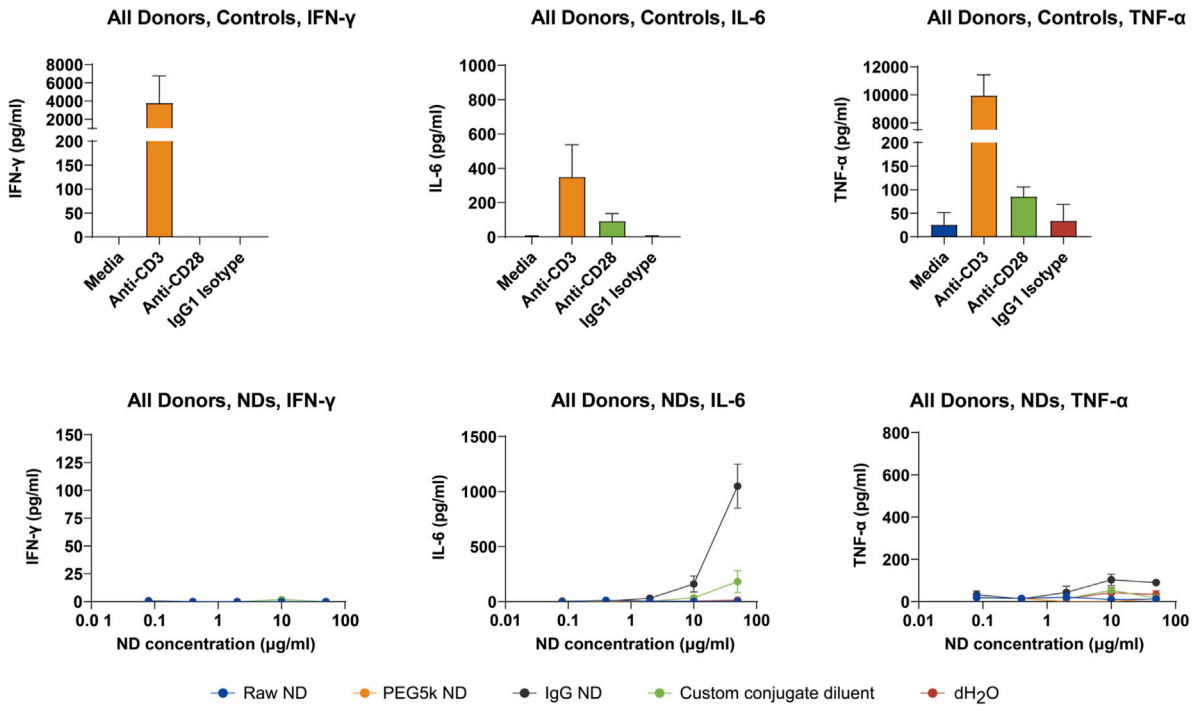

FIGURE 3
Cytokine responses in PBMC culture supernatants.

were treated with anti-CD3 stimulation, there was a consistent increase in IL-6 secretion. IL-6 secretion was also induced, albeit to a much lesser degree, in cells treated with anti-CD28 stimulation. TNF-α was detectable at very low concentrations in supernatants from PBMCs from donors treated with media alone or isotype control (Figure 3; top-right panel). When cells were treated with anti-CD3 stimulation, there was a strong induction of TNF-α secretion in all three donors. Anti-CD28 stimulation trended towards an increase in TNF-α secretion, although at a factor approximately 10-fold lower than anti-CD3.

When PBMCs were incubated with NDs or vehicle, there was no detectable induction of IFN-γ under any condition (Figure 3; bottom-left panel). This suggests there was no specific activation of T or B cells in the PBMCs when tested under these conditions. There was an increase in IL-6 secretion in cells treated with the two highest doses of IgG-NDs (Figure 3; bottom-center panel). This was also apparent in the vehicle at the same concentrations, although to a lesser extent. This result, combined with the ATP data, suggests there may have been cell activation associated with non-specific cytotoxicity when the custom conjugate diluent was tested at 10%, as

well as when the IgG-NDs were tested at 50 μg/mL. This was also evidenced by the modest increase in TNF-α secretion at the highest concentrations of the IgG-NDs (Figure 3; bottom-right panel). Mean cytokine concentrations are presented below. Cytokine concentrations from individual donors are presented in Supplementary Data.

Displayed are the cytokine concentrations (IFN-γ, IL-6, and TNF-α) measured in supernatants from PBMC cultures of three healthy donors. The top panels represent controls, and the bottom panels show results following incubation with different ND formulations. Results highlight the selective cytokine secretion patterns in response to specific ND treatments, pointing towards their immunomodulatory potential. Each point is the mean of triplicate measures, with error bars indicating SEM. Custom conjugant dilutant consisted of 1*PBS +10% FBS; (see Section 2.2). Abbreviations: dH2O = sterile, filtered deionized water; h = hour; ND = nanodiamond; PBMC = peripheral blood mononuclear cells; SEM = standard error of the mean.

4 Discussion

4.1 Interpretation of results

Taken together, these data suggest the experiment yielded valid results, with findings for the controls falling within expected ranges and performing more favorably than detonation NDs (DNDs) (Mytych et al., 2015). Using ATP levels and cytokine concentrations as surrogates for cytotoxicity and immunogenicity, respectively, NDs conjugated to IgG induced inflammation at concentrations of 10 and 50 μg/mL. There was no induction of inflammation in PBMCs from the three healthy donors when incubated with raw-NDs, PEG5k-NDs, or IgG-NDs at 0.08, 0.4 or 2 μg/mL. Additionally, raw-NDs and PEG5k-NDs were well tolerated at concentrations up to 10 μg/mL.

The dose-dependent increase in ATP concentration up to 10 μg/mL across all LND formulations suggests an enhancement in cellular metabolic activity without inducing cytotoxic effects, indicative of the high biocompatibility of LNDs (Pentecost et al., 2017). However, the minimal changes in ATP levels at the highest concentration tested (50 μg/mL) hint at a cytotoxic threshold, aligning with ATP's dual role as both an energy source and a signaling molecule for cellular distress (Zimmermann, 2000; Vultaggio-Poma et al., 2020). The design of this study made it impossible to determine whether the effects observed at 50 μg/mL were caused by the IgG-NDs or exacerbated by the custom conjugate diluent. The results do suggest the custom conjugate diluent is well tolerated at concentrations of ≤0.4% but may have a deleterious effect on cell viability at concentrations of ≥2%. These effects might be caused by non-specific cytotoxicity, which is common in several vehicles tested at this concentration (Park et al., 2010; Sun et al., 2011; Kim et al., 2012; Qu et al., 2012; Crisponi et al., 2017; Lategan et al., 2018; Medici et al., 2021; Abuzreda and Yousif, 2023).

Differential cytokine responses to LND formulations, particularly the elevated secretion of IL-6 and TNF-α at higher concentrations of IgG-NDs, point to immune activation that could be influenced by surface chemistry and conjugation. The more pronounced responses in the presence of IgG-NDs suggest antibody conjugation could potentiate LND immunogenicity, possibly through specific targeting of immune cell receptors or enhanced nanoparticle uptake (Mochalin et al., 2012). This finding underscores the importance of surface modifications in designing nanodiamonds for biomedical applications, as these modifications can significantly influence immunological interactions (Kaur and Badea, 2013)

The strong IFN-γ and TNF-α response to anti-CD3 suggests the cell populations present, most likely T-cells, were sensitive to specific activation. Conversely, the low concentrations of IL-6 following anti-CD3 stimulation suggest controls had no appreciable effect on monocytes. This is further evidenced by the PBMCs' modest cytokine responses to anti-CD28 stimulation alone, which reinforces the conclusion there was no significant cellular activation under these conditions.

Whether PBMCs were incubated with NDs or vehicle, there was no detectable induction of IFN-γ under any condition, suggesting there was no specific activation of T- or B-cells in the PBMCs. Notably, the absence of a significant IFN-γ response across all conditions highlights the specificity of immune modulation induced by LNDs. IFN-γ is a key mediator of adaptive immunity, and its lack of induction suggests that LNDs may primarily influence innate immune mechanisms, offering potential pathways for enhancing anti-tumor immunity or mitigating autoimmune reactions without widespread activation of adaptive immune cells (Yuan et al., 2010)

However, incubation with IgG-NDs led to an increase in IL-6 secretion at higher doses (i.e., 10 and 50 μg/mL). The increase in IL-6 secretion at the highest concentrations tested suggests a pro-inflammatory response, warranting further investigation into the role of nanoparticle size, surface charge, and coating in modulating immune responses, as well as the potential contributory effects of certain diluents (Fadeel and Garcia-Bennett, 2010; Tsai et al., 2016). These observations are crucial for understanding how LNDs might be harnessed to modulate immune responses in therapeutic settingsWhile some of this increase may be attributable to the vehicle, the increases were larger in the IgG-ND group than in the vehicle controls. When considered within the context of the ATP data, it is reasonable to conclude there may have been cell activation associated with non-specific cytotoxicity when the custom conjugate diluent was tested at 10%, as well as when the IgG NDs were tested at 50 μg/mL. This was also evidenced by the modest increase in TNF-α secretion at the highest concentrations of the IgG-NDs.

A very strong positive correlation was observed between ATP production and IFN-γ levels (Pearson correlation coefficient = 0.979), with a statistically significant p-value of 0.021. This indicates that treatments leading to increased ATP production also tend to increase IFN-γ levels, suggesting a link between cellular metabolic activity and the immune response mediated by IFN-γ. Similarly, a very strong positive correlation was found between ATP production and TNF-α levels (Pearson correlation coefficient = 0.992), with a p-value of 0.008, indicating statistical significance. This result suggests that higher ATP production is associated with elevated TNF-α levels, further supporting the relationship between cellular energy levels and immune function, particularly the inflammatory response.

4.2 Comparison with existing literature

Comparatively, existing literature on nanodiamond applications in biomedicine has predominantly focused on detonation nanodiamonds (DNDs) and high-pressure high-temperature (HPHT) nanodiamonds. However, the synthesis methods for DNDs and HPHT NDs often result in a broader size distribution and potential for impurities (Baidakova et al., 2013; Tsai et al., 2016), which can influence their biocompatibility and immune interactions. Our study's emphasis on LNDs, with their consistent size (<5 nm) and high purity, underscores their potential to offer more controlled interactions with biological systems, thereby minimizing unintended immune responses.

Furthermore, previous studies, such as those by Mytych et al., 2015; Lategan et al., 2018, have underscored the critical influence of nanoparticle surface chemistry on their immunogenicity and cytotoxicity (Mytych et al., 2015; Lategan et al., 2018). Our observations that IgG-conjugated LNDs induce pro-inflammatory responses at higher concentrations further emphasize the delicate balance between nanoparticle functionalization and their immune compatibility, an aspect crucial for their application in targeted therapy.

This study also contributes to the ongoing discussion on nanodiamond biocompatibility and functionalization for biomedical applications. By focusing on LNDs, we elucidate how synthesis methods and surface conjugations impact their immunological interactions, providing a comparative analysis that enriches the existing literature on nanodiamonds' therapeutic potential in biomedicine (Sadat et al., 2022).

4.3 Enhanced biomedical applications of LNDs

Our study underscores the remarkable potential of laser-synthesized nanodiamonds (LNDs) in biomedical applications, highlighted by their high tolerance in peripheral blood mononuclear cells (PBMCs) without significant induction of inflammation or cytotoxicity. PEGylated LNDs stand out for drug delivery, offering improved biocompatibility and reduced immune response, which could enhance the delivery and efficacy of therapeutic agents (Turcheniuk and Mochalin, 2017; Gao et al., 2019). Additionally, antibody-conjugated LNDs highlight the precision medicine potential, targeting specific cells or tissues for therapeutic action while minimizing side effects (Suarez-Kelly et al., 2021; Paladhi et al., 2022). Their inherent fluorescence and biocompatibility also position LNDs as advantageous for bioimaging, facilitating the non-invasive monitoring of disease processes and therapeutic response (Perevedentseva et al., 2013).

4.4 Suggestions for future research

Exploring the role of nanoparticle surface chemistry in immune responses and the effects of LNDs on various components of the immune system will be vital for characterizing their immunomodulatory potential. Further studies should delineate the mechanisms underlying LNDs' dose-dependent effects on cellular metabolism and immune activation, optimizing LND design for specific biomedical applications (Stone et al., 2009; Mochalin et al., 2012).

In conclusion, this study contributes valuable insights into the immunomodulatory effects of LNDs on PBMCs, laying the groundwork for future investigations into the therapeutic potential of these nanomaterials. As we continue to unravel the complex interactions between nanodiamonds and the immune system, the promise of nanodiamond-based therapeutics in modulating immune responses for disease treatment and prevention becomes increasingly tangible.

Data availability statement

The original contributions presented in the study are included in the article/Supplementary Material, further inquiries can be directed to the corresponding author.

Ethics statement

Ethical approval was not required for the studies on humans in accordance with the local legislation and institutional requirements because only commercially available established cell lines were used.

Author contributions

EA: Writing–original draft, Writing–review and editing. KL: Writing–review and editing.

Funding

The author(s) declare that no financial support was received for the research, authorship, and/or publication of this article.

Conflict of interest

The authors declare that the research was conducted in the absence of any commercial or financial relationships that could be construed as a potential conflict of interest.

Publisher's note

All claims expressed in this article are solely those of the authors and do not necessarily represent those of their affiliated organizations, or those of the publisher, the editors and the reviewers. Any product that may be evaluated in this article, or claim that may be made by its manufacturer, is not guaranteed or endorsed by the publisher.

Supplementary material

The Supplementary Material for this article can be found online at: https://www.frontiersin.org/articles/10.3389/fnano.2024.1352287/full#supplementary-material

References

Abuzreda, A., and Yousif, A. (2023). *toxicity-of-iron-oxide-nanoparticles-on–antioxidant-enzymes-and-free-radicals-in-male-rats* 7, 140. doi:10.35841/aamsn-7.2.140

Alexander, A., Saraf, S., Saraf, S., Agrawal, M., Patel, R. J., Agrawal, P., et al. (2019). Amalgamation of stem cells with Nanotechnology: a unique therapeutic approach. *Curr. Stem Cell Res. Ther.* 14 (2), 83–92. doi:10.2174/1574888x13666180703143219

Ansari, S. A., Satar, R., Jafri, M. A., Rasool, M., Ahmad, W., and Kashif Zaidi, S. (2016). Role of nanodiamonds in drug delivery and stem cell therapy. *Iran. J. Biotechnol.* 14 (3), 130–141. doi:10.15171/ijb.1320

Baidakova, M. V., Kukushkina, Y. A., Sitnikova, A. A., Yagovkina, M. A., Kirilenko, D. A., Sokolov, V. V., et al. (2013). Structure of nanodiamonds prepared by laser synthesis. *Phys. Solid State* 55 (8), 1747–1753. doi:10.1134/s1063783413080027

Chang, S., Popowich, Y., Greco, R. S., and Haimovich, B. (2003). Neutrophil survival on biomaterials is determined by surface topography. *J. Vasc. Surg.* 37 (5), 1082–1090. doi:10.1067/mva.2003.160

Chang, S. L. Y., Reineck, P., Krueger, A., and Mochalin, V. N. (2022). Ultrasmall nanodiamonds: perspectives and questions. *ACS Nano* 16 (6), 8513–8524. doi:10.1021/acsnano.2c00197

Crisponi, G., Nurchi, V., Lachowicz, J., Peana, M., Medici, S., and Zoroddu, M. (2017). "Chapter 18 - toxicity of nanoparticles: etiology and mechanisms," in *Antimicrobial nanoarchitectonics*. Editor A. M. Grumezescu (Amsterdam, Netherlands: Elsevier), 511–546.

Di Virgilio, F., Sarti, A. C., and Grassi, F. (2018). Modulation of innate and adaptive immunity by P2X ion channels. *Curr. Opin. Immunol.* 52, 51–59. doi:10.1016/j.coi.2018.03.026

Fadeel, B., and Garcia-Bennett, A. E. (2010). Better safe than sorry: understanding the toxicological properties of inorganic nanoparticles manufactured for biomedical applications. *Adv. Drug Deliv. Rev.* 62 (3), 362–374. doi:10.1016/j.addr.2009.11.008

Gao, G., Guo, Q., and Zhi, J. (2019). Nanodiamond-based theranostic platform for drug delivery and bioimaging. *Small* 15 (48), e1902238. doi:10.1002/smll.201902238

Ghoneum, M. H., Pan, D., and Katano, H. (2014). *Enhancement of human T lymphocyte proliferation by nanodiamond and nanoplatinum in liquid. DPV576.*

Huang, K. J., Lee, C., Lin, Y., Lin, C., Perevedentseva, E., Hung, S., et al. (2017). Phagocytosis and immune response studies of Macrophage-Nanodiamond Interactions *in vitro* and *in vivo*. *J. Biophot.* 10 (10), 1315–1326. doi:10.1002/jbio.201600202

Iwamoto, T., Sugimoto, A., Kitamura, T., Akazawa, Y., and Hasegawa, T. (2014). The role of extracellular ATP-mediated purinergic signaling in bone, cartilage, and tooth tissue. *J. Oral Biosci.* 56 (4), 131–135. doi:10.1016/j.job.2014.07.003

Kaçar, C., and Erden, P. E. (2020). An amperometric biosensor based on poly(L-aspartic acid), nanodiamond particles, carbon nanofiber, and ascorbate oxidase-modified glassy carbon electrode for the determination of L-ascorbic acid. *Anal. Bioanal. Chem.* 412 (22), 5315–5327. doi:10.1007/s00216-020-02747-w

Kalyanaraman, B. (2017). Teaching the basics of cancer metabolism: developing antitumor strategies by exploiting the differences between normal and cancer cell metabolism. *Redox Biol.* 12, 833–842. doi:10.1016/j.redox.2017.04.018

Kaur, R., and Badea, I. (2013). Nanodiamonds as novel nanomaterials for biomedical applications: drug delivery and imaging systems. *Int. J. Nanomedicine* 8, 203–220. doi:10.2147/ijn.s37348

Kim, T. H., Kim, M., Park, H., Shin, U. S., Gong, M., and Kim, H. (2012). Size-dependent cellular toxicity of silver nanoparticles. *J. Biomed. Mater Res. A* 100 (4), 1033–1043. doi:10.1002/jbm.a.34053

Lategan, K., Alghadi, H., Bayati, M., de Cortalezzi, M., and Pool, E. (2018). Effects of graphene oxide nanoparticles on the immune system biomarkers produced by RAW 264.7 and human whole blood cell cultures. *Nanomater. (Basel)* 8 (2), 125. doi:10.3390/nano8020125

Li, C., Luo, S. X. L., Kim, D. M., Wang, G., and Cappellaro, P. (2023). Ion sensors with crown ether-functionalized nanodiamonds. Available at: https://arxiv.org/abs/2301.03143.

Lin, Y. W., Su, H. C., Raj, E. N., Liu, K. K., Chang, C. J., Hsu, T. C., et al. (2022). Targeting EGFR and monitoring tumorigenesis of human lung cancer cells *in vitro* and *in vivo* using nanodiamond-conjugated specific EGFR antibody. *Pharmaceutics* 15 (1), 111. doi:10.3390/pharmaceutics15010111

Liu, C. Y., Lee, M. C., Lin, H. F., Lin, Y. Y., Lai, W. Y., Chien, Y., et al. (2021). Nanodiamond-based microRNA delivery system promotes pluripotent stem cells toward myocardiogenic reprogramming. *J. Chin. Med. Assoc.* 84 (2), 177–182. doi:10.1097/jcma.0000000000000441

Medici, S., Peana, M., Pelucelli, A., and Zoroddu, M. A. (2021). An updated overview on metal nanoparticles toxicity. *Seminars Cancer Biol.* 76, 17–26. doi:10.1016/j.semcancer.2021.06.020

Mochalin, V. N., Shenderova, O., Ho, D., and Gogotsi, Y. (2012). The properties and applications of nanodiamonds. *Nat. Nanotechnol.* 7 (1), 11–23. doi:10.1038/nnano.2011.209

Montes, R., Sánchez, G., Zhao, J., Palet, C., Baeza, M., and Bastos-Arrieta, J. (2020). Customized *in situ* functionalization of nanodiamonds with nanoparticles for composite carbon-paste electrodes. *Nanomaterials* 10 (6), 1179. doi:10.3390/nano10061179

Mytych, J., Lewinska, A., Zebrowski, J., and Wnuk, M. (2015). Nanodiamond-induced increase in ROS and RNS levels activates NF-κB and augments thiol pools in human hepatocytes. *Diam. Relat. Mater.* 55, 95–101. doi:10.1016/j.diamond.2015.03.014

Paladhi, A., Rej, A., Sarkar, D., Singh, R., Bhattacharyya, S., Sarkar, P. K., et al. (2022). Nanoscale diamond-based formulation as an immunomodulator and potential therapeutic for lymphoma. *Front. Pharmacol.* 13, 852065. doi:10.3389/fphar.2022.852065

Park, E. J., Kim, H., Kim, Y., Yi, J., Choi, K., and Park, K. (2010). Carbon fullerenes (C60s) can induce inflammatory responses in the lung of mice. *Toxicol. Appl. Pharmacol.* 244 (2), 226–233. doi:10.1016/j.taap.2009.12.036

Peer, D., Zhu, P., Carman, C. V., Lieberman, J., and Shimaoka, M. (2007). Selective gene silencing in activated leukocytes by targeting siRNAs to the integrin lymphocyte function-associated antigen-1. *Proc. Natl. Acad. Sci. U. S. A.* 104 (10), 4095–4100. doi:10.1073/pnas.0608491104

Pentecost, A., Kim, M. J., Jeon, S., Ko, Y. J., Kwon, I. C., Gogotsi, Y., et al. (2019). Immunomodulatory nanodiamond aggregate-based platform for the treatment of rheumatoid arthritis. *Regen. Biomater.* 6 (3), 163–174. doi:10.1093/rb/rbz012

Pentecost, A. E., Witherel, C. E., Gogotsi, Y., and Spiller, K. L. (2017). Anti-inflammatory effects of octadecylamine-functionalized nanodiamond on primary human macrophages. *Biomaterials Sci.* 5 (10), 2131–2143. doi:10.1039/c7bm00294g

Perevedentseva, E., Lin, Y. C., Jani, M., and Cheng, C. L. (2013). Biomedical applications of nanodiamonds in imaging and therapy. *Nanomedicine* 8 (12), 2041–2060. doi:10.2217/nnm.13.183

Perevedentseva, E., Peer, D., Uvarov, V., Zousman, B., and Levinson, O. (2015). Nanodiamonds of laser synthesis for biomedical applications. *J. Nanosci. Nanotechnol.* 15 (2), 1045–1052. doi:10.1166/jnn.2015.9747

Qu, C., Wang, L., He, J., Tan, J., Liu, W., Zhang, S., et al. (2012). Carbon nanotubes provoke inflammation by inducing the pro-inflammatory genes IL-1β and IL-6. *Gene* 493 (1), 9–12. doi:10.1016/j.gene.2011.11.046

Reina, G., Zhao, L., Bianco, A., and Komatsu, N. (2019). Chemical functionalization of nanodiamonds: opportunities and challenges ahead. *Angew. Chem. Int. Ed.* 58 (50), 17918–17929. doi:10.1002/anie.201905997

Sadat, Z., Farrokhi-Hajiabad, F., Lalebeigi, F., Naderi, N., Ghafori Gorab, M., Ahangari Cohan, R., et al. (2022). A comprehensive review on the applications of carbon-based nanostructures in wound healing: from antibacterial aspects to cell growth stimulation. *Biomater. Sci.* 10 (24), 6911–6938. doi:10.1039/d2bm01308h

Shao, D., Li, M., Wang, Z., Zheng, X., Lao, Y., Chang, Z., et al. (2018). Bioinspired diselenide-bridged mesoporous silica nanoparticles for dual-responsive protein delivery. *Adv. Mater.* 30 (29), 1801198. doi:10.1002/adma.201801198

Sharmin, R., Nusantara, A. C., Nie, L., Wu, K., Elias Llumbet, A., Woudstra, W., et al. (2022). Intracellular quantum sensing of free-radical generation induced by acetaminophen (APAP) in the cytosol, in mitochondria and the nucleus of macrophages. *ACS Sensors* 7 (11), 3326–3334. doi:10.1021/acssensors.2c01272

Stone, V., Johnston, H., and Schins, R. P. (2009). Development of *in vitro* systems for nanotoxicology: methodological considerations. *Crit. Rev. Toxicol.* 39 (7), 613–626. doi:10.1080/10408440903120975

Suarez-Kelly, L. P., Campbell, A. R., Rampersaud, I. V., Bumb, A., Wang, M. S., Butchar, J. P., et al. (2017). Fluorescent nanodiamonds engage innate immune effector cells: a potential vehicle for targeted anti-tumor immunotherapy. *Nanomedicine Nanotechnol. Biol. Med.* 13 (3), 909–920. doi:10.1016/j.nano.2016.12.005

Suarez-Kelly, L. P., Sun, S. H., Ren, C., Rampersaud, I. V., Albertson, D., Duggan, M. C., et al. (2021). Antibody conjugation of fluorescent nanodiamonds for targeted innate immune cell activation. *ACS Appl. Nano Mater* 4 (3), 3122–3139. doi:10.1021/acsanm.1c00256

Sun, Z., Liu, Z., Meng, J., Meng, J., Duan, J., Xie, S., et al. (2011). Carbon nanotubes enhance cytotoxicity mediated by human lymphocytes *in vitro*. *PLoS One* 6 (6), e21073. doi:10.1371/journal.pone.0021073

Taylor, A. C., González, C. H., Ferretti, P., and Jackman, R. B. (2019). Spontaneous differentiation of human neural stem cells on nanodiamonds. *Adv. Biosyst.* 3 (4), e1800299. doi:10.1002/adbi.201800299

Tsai, L. W., Lin, Y. C., Perevedentseva, E., Lugovtsov, A., Priezzhev, A., and Cheng, C. L. (2016). Nanodiamonds for medical applications: interaction with blood *in vitro* and *in vivo*. *Int. J. Mol. Sci.* 17 (7), 1111. doi:10.3390/ijms17071111

Turcheniuk, K., and Mochalin, V. N. (2017). Biomedical applications of nanodiamond (Review). *Nanotechnology* 28 (25), 252001. doi:10.1088/1361-6528/aa6ae4

van der Laan, K. J., Morita, A., Perona-Martinez, F. P., and Schirhagl, R. (2020). Evaluation of the oxidative stress response of aging yeast cells in response to internalization of fluorescent nanodiamond biosensors. *Nanomater. (Basel)* 10 (2), 372. doi:10.3390/nano10020372

Vultaggio-Poma, V., Sarti, A. C., and Di Virgilio, F. (2020). Extracellular ATP: a feasible target for cancer therapy. *Cells* 9 (11), 2496. doi:10.3390/cells9112496

Yuan, Y., Wang, X., Jia, G., Liu, J. H., Wang, T., Gu, Y., et al. (2010). Pulmonary toxicity and translocation of nanodiamonds in mice. *Diam. Relat. Mater.* 19 (4), 291–299. doi:10.1016/j.diamond.2009.11.022

Zimmermann, H. (2000). Extracellular metabolism of ATP and other nucleotides. *Naunyn Schmiedeb. Arch. Pharmacol.* 362 (4-5), 299–309. doi:10.1007/s002100000309